Coordination Environment and Vibrational Spectroscopy of Cr(VI) Sites Supported on Amorphous Silica

Cristina Moisii,[†] Eric W. Deguns,[‡] Adrian Lita,[†] Sean D. Callahan,[†] Lambertus J. van de Burgt,[†] Donny Magana,[†] and A. E. Stiegman*[,†,§]

Department of Chemistry and Biochemistry and The Materials Research and Technology Center (MARTECH), Florida State University, Tallahassee, Florida 32306 and Department of Chemistry and Chemical Engineering, University of California, Santa Barbara, California 93106-5080

Received January 18, 2006. Revised Manuscript Received May 17, 2006

Chromium(VI) sites homogeneously dispersed in a transparent silica xerogel matrix have been investigated to determine the coordination environment and rationalize the Raman spectra. X-ray absorption fine structure (EXAFS) analysis gives a structure that is consistent with Cr containing two terminal oxygens and is bound to the silica by two Cr−O−Si linkages. The structure was refined to an *R* factor of 1.28%. The terminal Cr═O bonds were found to have a bond length of 1.60 Å and bridging Cr−O bonds of 1.80 Å. The Raman spectrum, collected with 785 nm excitation above the absorption edge of the chromium, shows a strong band at 986 cm^{-1} and a resolved shoulder at 1001 cm^{-1}. Isotopic labeling and polarization studies of low concentrations of Cr (0.5 mol %) indicate that the strong 986 cm^{-1} band is the totally symmetric $Cr(═O)_2$ mode; however, the isotopic shift and strong polarization of the 1001 cm^{-1} mode preclude it from being the antisymmetric component of the terminal dioxo stretch. At higher concentrations (≤5.0 mol %) the high-energy shoulder becomes a resolved peak at 1004 cm^{-1}. While isotopic labeling shifts the peak to a position predicted for the antisymmetric stretch, the polarization ratio increases but does not reach a value that is unambiguous for an antisymmetric mode.

Introduction

The structure of Cr(VI) oxide sites dispersed at monolayer or submonolayer coverage on a silica support is of interest as a precursor to the Phillips polymerization catalyst which is subsequently formed from reduction of these sites with either ethylene or carbon monoxide.[1,2] The structure of Cr(VI) bound to a silica surface is often written as a dioxo species (Figure 1a) with two terminal Cr═O bonds and two Si−O−Cr bridges. This structure, which is nominally derived from known small molecule analogues such as chromyl chloride and from structures believed to result from proposed grafting reactions, has become ubiquitous in the literature and is the starting point for most discussions of the generation of the Phillips catalyst.[2] Notwithstanding this, there is little direct experimental evidence supporting this structure and much of the available data can easily support plausible alternative structures with higher coordination environments such as that shown in Figure 1b.

There have been several approaches to characterizing the structure of isolated Cr(VI) sites on silica including, but not exclusively, vibrational spectroscopy and X-ray absorption studies (EXAFS). In the case of vibrational spectroscopy, and in particular Raman spectroscopy, studies aimed at positively identifying the dioxo site through observation of both the symmetric and antisymmetric $Cr(═O)_2$ stretching modes that would necessarily accompany such a group have been reported. Early Raman studies by Wachs et al. on dehydrated Cr on silica resolved a single line at 986 cm^{-1} which was assigned, by reference to small molecule analogues and through ^{18}O-labeling studies, to a terminal Cr═O stretch. Under ambient (hydrous) conditions and at higher loadings of Cr other bands are ultimately observed and were assigned to, among other things, dimeric and oligomeric chromate species.[3−5] This work, while providing valuable insights into the surface chemistry of silica-supported chromium, did not resolve a mode assignable to the antisymmetric stretch in an isolated Cr(VI) site. More recently, Dines and Inglis carried out careful density functional calculations on cluster models of the CrO_2 site and predicted that the antisymmetric stretch should be observed at 1010 cm^{-1}.[6] Raman spectra reported by these authors and a more

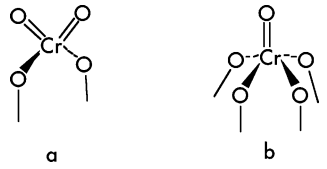

Figure 1.

* To whom correspondence should be addressed. Phone: 850-644-6605. E-mail: Stiegman@chem.fsu.edu.
[†] Department of Chemistry and Biochemistry, Florida State University.
[‡] Department of Chemistry and Chemical Engineering, University of California,
[§] The Materials Research and Technology Center, Florida State University.

(1) Groppo, E.; Lamberti, C.; Bordiga, S.; Spoto, G.; Zecchina, A. *Chem. Rev.* **2005**, *105*, 115−183.
(2) McDaniel, M. P. *Adv. Catal.* **1985**, *33*, 47−98.
(3) Vuurman, M. A.; Wachs, I. E.; Stufkens, D. J.; Oskam, A. *J. Mol. Catal.* **1993**, *80*, 209−227.
(4) Hardcastle, F. D.; Wachs, I. E. *J. Mol. Catal.* **1988**, *46*, 173−186.
(5) Weckhuysen, B. M.; Wachs, I. E. *J. Phys. Chem. B* **1997**, *101*, 2793−2796.
(6) Dines, T. J.; Inglis, S. *Phys. Chem. Chem. Phys.* **2003**, *5*, 1320−1328.

10.1021/cm0601281 CCC: $33.50
Published on Web 08/01/2006

recent study by Groppo et al. resolve a high-energy shoulder on the 990 cm^{-1} symmetric stretch at ~1004 cm^{-1} which, based on the Dines and Inglis calculations, has been assigned as the antisymmetric stretch.[1,7] Assignments based solely on calculations of small cluster analogues are not spectroscopically rigorous and can only be viewed as guides to expected energy of specific modes. As such, this band cannot, at this juncture, be viewed as diagnostic of a silica-bound CrO_2 unit.

X-ray absorption studies (XANES and EXAFS) have been carried out by several groups on both oxidized and reduced silica-supported Cr. Earlier studies by Weckhuysen et al. and a more recent study by Groppo et al. deduced evidence for both short and long chromium−oxygen bonds, but in both cases relatively large concentrations of Cr were deposited (4 wt %) and evidence of more complex oligomeric species was also observed.[8,9] Wang et al. reported the results of an X-ray absorption study of dilute (1 and 2 mol %) dispersions of Cr in MCM-41. The best fit of the EXAFS for the isolated Cr sites was to a four-coordinate species with two short and two long chromium−oxygen bonds.[10] While this study is somewhat more compelling due to the lower concentrations of Cr, negative values of the Debye−Waller factors were reported in parameters of the best fits to the data. Negative values are nonphysical, and since the Debye−Waller factors are highly correlated with the coordination number, it still affords the possibility that a higher coordination number species may be correct.

In past studies of silica-supported metal oxides we dispersed the metals of interest in transparent monoliths of high optical quality made through the sol−gel process.[11] This matrix provides a superior medium for both electronic absorption/emission and Raman spectroscopic studies, yielding spectra of much better signal to noise than can be obtained from diffusely scattering powders. In addition, since they are isotropic and nonscattering, accurate polarization ratios can be obtained to assist in spectroscopic assignments. Finally, the enhanced sensitivity of the transparent medium allows interrogation of very dilute systems where the metal sites are isolated. These properties have been exploited with great success for spectroscopic characterization of the vanadium and titanium sites in silica.[12−15] In this study we prepare a series of Cr−silica xerogels with concentrations ranging from 0.5 to 5 mol % Cr. We exploited this series to characterize the coordination environment of the discrete Cr(VI) site. In particular, X-ray absorption data of dilute samples have been collected at low temperatures in fluorescence mode. Fits of these data to plausible structural models establish with considerable certainty that the dioxo site is the predominant species at low concentration. Finally, the Cr−silica xerogel monoliths were used to obtain well-resolved Raman spectra for which spectroscopic assignments can be made. This study rationalizes both the structure and spectroscopy of the isolated Cr(VI) site.

Experimental Section

Xerogel Synthesis. Chromium−silica xerogel monoliths were made by adapting a previously published technique.[11,12] Sols were made by addition of an alcoholic solution of TMOS and the necessary quantity of chromic acid to a water/ethanol mixture. Stock solution of chromic acid was made using 99.9% chromium(VI) oxide (Aldrich) and deionized water (10^{-18} Ω; Barnsted E-Pure system). To obtain homogeneous mixtures, all solutions were sonicated for 5 min. Aliquots of 4 mL of the sol were dispensed into 1 cm styrene cuvettes, sealed, and allowed to gel. Caps were removed after gelation and allowed to age and evaporate for about 3−4 months. The samples were then dried in a programmable furnace. They were initially ramped to 100 °C at a rate of 0.5 °C/h, where they were allowed to dry for 72 h. They were then ramped at the same rate to 500 °C, where they were maintained for 36 h. Finally, they were cooled back to room temperature over a period of 95 h. Materials containing up to 5 mol % chromium [(Cr/Cr + Si) × 100] were made following this procedure. The BET surface area of a typical 0.5 mol % calcined Cr−silica xerogel was found to be 335 m^2/g.

Isotopic Labeling. ^{18}O was incorporated into the samples through a series of reduction/oxidation cycles that utilize isotopically enriched $^{18}O_2$ in the oxidation step. The chromium−silica monoliths were reduced in a tube furnace under a flow of CO for 3 h at 230 °C. Reduction at higher temperatures (i.e., >300 °C), which is often used to generate the Phillips catalyst, was found to yield residual fluorescence in the matrix, which interfered with Raman spectroscopy. At the completion of the reduction process the monolith was transferred in an inert environment to a high-pressure bomb where it was pressurized with 125 psi of $^{18}O_2$ (Isotec, 97 atom %). Oxidation was carried out at 530 °C for a period of 24 h. Up to five reduction/oxidation cycles were performed on the samples to achieve the isotopic incorporation reported. Raman spectra were collected between redox cycles to assess the degree of isotopic substitution with great care being taken to see that the samples were not exposed to ambient conditions at any time during that process.

XAS Spectroscopy. X-ray absorption spectroscopy was performed at the Stanford Synchrotron Radiation Laboratory (SSRL) on beamline BL2-3 (Bend). X-rays were monochromatized via reflection from Si(111) crystals through a 1 mm entrance slit. The incident beam was detuned (40−50%) to suppress harmonics. The intensity of the X-ray beam was measured with N_2-filled ion chamber detectors. Powdered samples of 0.5 mol % Cr−silica xerogel materials were loaded under anhydrous conditions into an aluminum sample holder (10 × 4 × 2 mm window) between sealed layers of 12.0 μm polypropylene film (Chemplex #475). Spectra were collected in fluorescence mode due to the low concentration of Cr sites present. Fluorescence was recorded with an Ar-purged Lytle detector without Soller slits. To suppress thermal motion, the spectra were collected at 20 K in an Oxford Instruments liquid He flow cryostat. Multiple sweeps were collected and averaged for an improved signal-to-noise ratio.

XAS Data Analysis. Energy calibration was performed using the spectrum of the Cr-calibrated foil (5989.2 eV K-edge) recorded

(7) Groppo, E.; Damin, A.; Bonino, F.; Zecchina, A.; Bordiga, S.; Lamberti, C. *Chem. Mater.* **2005**, *17*, 2019−2027.
(8) Groppo, E.; Prestipino, C.; Bonino, F.; Bordiga, S.; Lamberti, C.; Thune, P. C.; Niemantsverdriet, J. W.; Zecchina, A. *J. Catal.* **2005**, *230*, 98−108.
(9) Weckhuysen, B. M.; Schoonheydt, R. A.; Jehng, J. M.; Wachs, I. E.; Cho, S. J.; Ryoo, R.; Kijlstra, S.; Poels, E. *J. Chem. Soc., Faraday Trans.* **1995**, *91*, 3245−3253.
(10) Wang, Y.; Ohishi, Y.; Shishido, T.; Zhang, Q. H.; Yang, W.; Guo, Q.; Wan, H. L.; Takehira, K. *J. Catal.* **2003**, *220*, 347−357.
(11) Stiegman, A. E.; Eckert, H.; Plett, G.; Kim, S. S.; Anderson, M.; Yavrouian, A. *Chem. Mater.* **1993**, *5*, 1591−1594.
(12) Curran, M. D.; Gedris, T. E.; Stiegman, A. E.; Plett, G. A. *Chem. Mater.* **1999**, *11*, 1120−1127.
(13) Soult, A. S.; Carter, D. F.; Schreiber, H. D.; van de Burgt, L. J.; Stiegman, A. E. *J. Phys. Chem. B* **2002**, *106*, 9266−9273.
(14) Tran, K.; Hanninglee, M. A.; Biswas, A.; Stiegman, A. E.; Scott, G. W. *J. Am. Chem. Soc.* **1995**, *117*, 2618−2626.
(15) Tran, K.; Stiegman, A. E.; Scott, G. W. *Inorg. Chim. Acta* **1996**, *243*, 185−191.

simultaneously for each sample.[16] Data reduction and analysis was accomplished using WinXAS (v. 3.1).[17] Spectra were background corrected by subtracting a linear fit to the preedge region, which was extrapolated to the length of the entire spectrum, then normalized by eighth degree polynomial fit to the postedge region. After normalization, the EXAFS spectra were k^3-weighted and fitted with a seven-knot polynomial spline between 1.0 and 13.8 $Å^{-1}$, which was subtracted to decrease contributions from atomic X-ray absorption fine structure.[18] A Bessel window was applied to the first and last 4% of the data prior to Fourier transformation to R space. The scattered wave properties for each trial structure were calculated using FEFF 8.2.[19,20] EXAFS fits were carried out by systematically refining the bond lengths, R, Debye−Waller factors, σ^2, and inner potential corrections, ΔE_0, for the models considered. EXAFS fits were first performed on k^3-weighted data and verified for consistency against k^1-weighted data. XANES preedge peak heights and positions were computed with a least-squares fit using an Arctan function for the normalized K-edge and a Lorenzian function for the prepeak. Obtained values were subsequently checked against a first-derivative plot. The quality of the structure was assessed by checking the plausibility of obtained values, comparing the residuals and statistical tests. The residuals (eq 1), where χ_{obs} and χ_{calc} are the experimental and calculated EXAFS curves, respectively, were calculated by WinXAS.

$$R = \frac{\sum_{i=1}^{N} |\chi_{obs}(k_i) - \chi_{calc}(k_i)|}{\sum_{i=1}^{N} |\chi_{obs}(k_i)|} \times 100 \quad (1)$$

The statistical tests were identical to those performed elsewhere.[21]

UV−Vis Absorption and Emission Spectroscopy. Absorption spectra were collected in transmission mode through 0.005 and 0 mol % Cr−Silica xerogel monoliths on a Perkin-Elmer Lambda 900 spectrophotometer. Emission spectra were collected on a Spex Fluorolog τ-2 equipped with 250 mm single monochromators. Excitation was at 351 nm from a Coherent I-308 argon-ion laser. The excitation and emission slits were 0.5 nm. In all cases the samples were baked at 500 °C under an oxygen flow and then transferred directly into an antechamber, where they are placed in spectroscopic cells which were then evacuated prior to collecting data.

Raman Spectroscopy. Raman spectra were obtained using a micro/Raman spectrograph, JY Horiba LabRam HR800, excited by a TUI Optics DL 100 grating-stabilized diode laser emitting 80 mW of power at 785 nm. The power at the sample was 6 mW. The spectrograph uses a holographic notch filter to couple the laser beam into the microscope (Olympus BX30) by total reflection. The beam is focused on the sample through a microscope objective 5× (Olympus N. A. 0.10). Backscattered radiation is collected by the objective, and laser radiation is filtered out by the notch filter with Raman scattering coupled into the spectrograph through a confocal hole. A 76 mm square 600 line/mm grating disperses the Raman scatter onto a 1024 × 256 element open electrode CCD detector (Wright CCD30-11-0-275) having 26 μm square pixels thermoelectrically cooled to −70 °C. The detector has a quantum efficiency of 45−22% in the range of 785−900 nm.

Polarization ratios (I_{HV}/I_{HH}) were calculated from the integrated intensity of the peaks obtained from Raman spectra in which the scattered radiation was collected parallel (I_{HH}) and perpendicular (I_{HV}) to the polarization of the excitation beam. Overlapping bands were deconvoluted into Gaussian−Lorentzian peaks using JY Horiba Labspec (v. 4.02) software, and the ratios of the resulting peak areas were used to calculate the polarization ratio. Only deconvolution analysis that generated spectroscopically resolved peaks were considered valid. No peak positions or peak areas were used from spectral deconvolution that generated additional, unobserved peaks in the analysis.

Simulated Raman spectra were calculated using the Vibratz (version 2.0) normal coordinate analysis program (Shape Software, Inc.). Calculations were performed on a model structure, $(Si-O-)_2CrO_2$, using the bond lengths, angles, and scaled force constants reported by Dines and Inglis (Tables 3 and 5, ref 6). The force constants for the stretching and bending of the $Cr(=O)_2$ unit were adjusted to bring the calculated symmetric and antisymmetric stretching frequencies into agreement with 986 and 1001 cm^{-1} bands observed experimentally. The bandwidths plotted in the simulation were adjusted to bring them into agreement with the experimentally observed bandwidth.

FT-IR Spectroscopy. FT-IR spectra of homogeneous xerogels containing chromium loadings up to 5 mol % were collected on an Avatar 360 E.S.P. spectrometer using Nicolet's Omnic software. The chromium monoliths were ground with the KBr (Fisher, IR grade) in a dilution of 5% sample and 95% KBr. The samples were never exposed to ambient conditions. FT-IR spectroscopy was carried out in a stainless steel reaction chamber with a stainless steel dome used in conjunction with a Harrick Scientific Praying Mantis Diffuse Reflection Attachment. Argon (UHP grade) was continuously introduced into the sample cup and diffused through the sample. The FT-IR spectrometer itself was placed in an inert atmosphere chamber, which was continuously flushed with Ar in order for the samples to remain dry.

Results and Discussion

Structure of the Cr(VI) Site. The X-ray absorption near-edge (XANES) spectrum, collected in fluorescence mode at 15 K, of a 1.0 mol % Cr−silica xerogel is shown in Figure 2a. The preedge XANES region shows a single sharp peak with an intensity of 0.68, at 5991.7 eV, or 2.5 eV past the Cr metal edge. This peak is the 1s → 3d molecular absorption of the Cr(VI) sites.[8] Observation of a strongly allowed XANES transition for the Cr site indicates that the site is noncentrosymmetric, which is consistent with either of the proposed structures (1a or 1b) but does not permit differentiation between them. A previous study of the XANES regions of calcium−chromates concluded that a single, sharp preedge feature is characteristic of a tetrahedral chromium site.[22] The first-derivative representation shows maxima associated with the preedge feature in addition to the K-edge of the sample. The K-edge is located at 6007.5 eV (Δ = 18.3 eV), consistent with chromium being in a +6 oxidation

(16) Bearden, J. A. *Rev. Mod. Phys.* **1967**, *39*, 78-&.
(17) Ressler, T. *J. Synchrotron Radiat.* **1998**, *5*, 118−122.
(18) Wang, W. C.; Chen, Y. *Phys. Stat. Solid A* **1998**, *168*, 351−357.
(19) Ankudinov, A. L.; Bouldin, C. E.; Rehr, J. J.; Sims, J.; Hung, H. *Phys. Rev. B* **2002**, *65*.
(20) Ankudinov, A. L.; Ravel, B.; Rehr, J. J.; Conradson, S. D. *Phys. Rev. B* **1998**, *58*, 7565−7576.
(21) Deguns, E. W.; Taha, Z.; Meitzner, G. D.; Scott, S. L. *J. Phys. Chem. B* **2005**, *109*, 5005−5011.
(22) Arcon, I.; Kodre, A. *In Materials Characterization by X-ray Absorption Spectroscopy (EXAFS, XANES)*, 36th International Conference on Microelectronics, Devices and Materials, Postojna, Slovenia, 2000; Postojna, Slovenia, 2000.

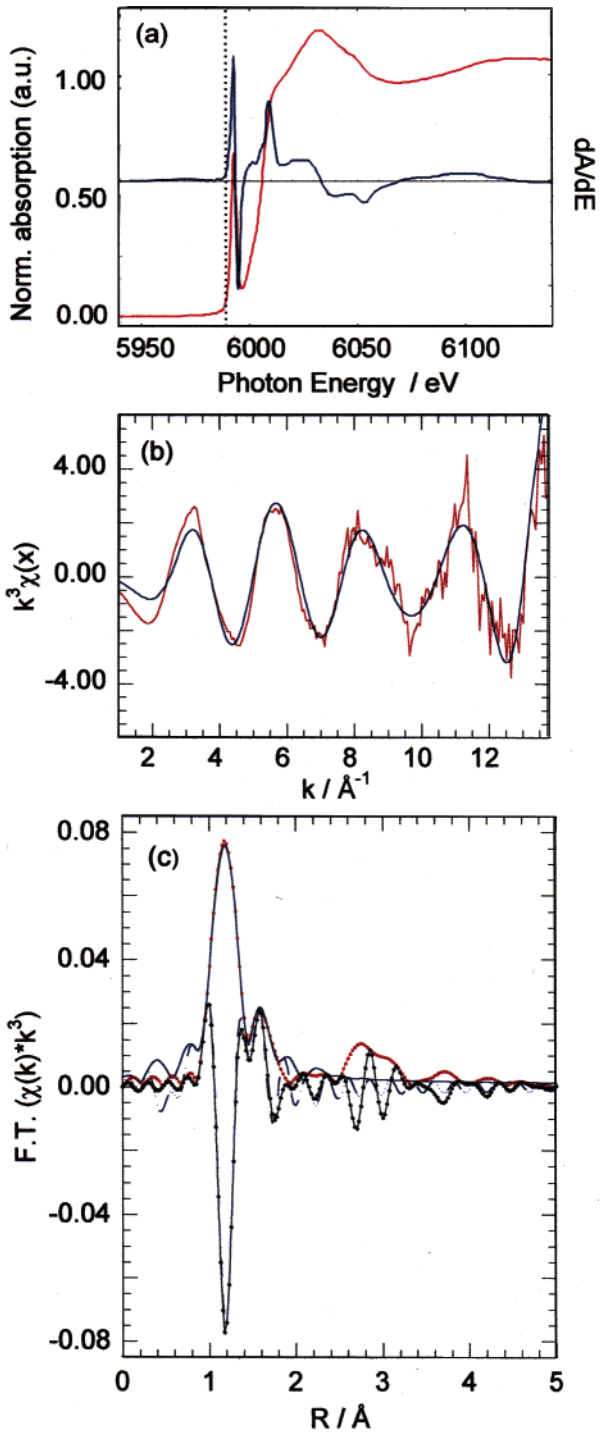

Figure 2. Cr K-edge XAS spectrum of 1% Cr−silica xerogel, recorded at 20 K. (a) XANES (red line) and first derivative (blue line). The Cr metal K-edge is marked at 5989.2 eV (dashed); (b) EXAFS in k^3-weighted k space (red line) and nonphase-corrected R space (imaginary data given as black points and FT magnitude as red points). The curve fit to the single-scattering model for the dioxo structure is shown (blue).

state.[22−24] The k^3-weighted EXAFS plotted in k and R space is shown in Figure 2b and 2c, respectively. Visual inspection of the R-space data shows two clearly resolvable peaks in early R. These are attributed to the chromium−oxo and chromium−siloxide paths.

Table 1. EXAFS Single-Scattering Fits[a] of a (≡SiO)Cr(═O)$_2$ Model with Refined and Fixed Coordination Numbers against Data of Cr(VI) Xerogel Sample, Recorded at 15 K

	refined N[b]				fixed N[c]			
path	N	R/Å	σ^2/Å^2	ΔE_0/eV	N	R/Å	σ^2/Å^2	ΔE_0/eV
Cr−O	2.14	1.60	0.00293	−2.13	2	1.60	0.00456	−0.51
Cr−O	1.83	1.79	0.00742	−2.13	2	1.80	0.00785	−0.51

[a] Errors for first-shell scattering fits calculated against EXAFS data, in the absence of systematic fitting uncertainties, are generally to be accepted as follows: bond lengths ±0.02 Å, σ^2 ± 20%, E_0 ±20%.[42] [b] $S_0^2 = 0.84$, residual = 16.37 for this model optimization. [c] $S_0^2 = 0.83$, residual = 18.18 for this model optimization.

To obtain bond length information the EXAFS was fitted for model structures with terminal and bridging oxygens in their first coordination sphere. Models consistent with both structures 1a and 1b were refined as was a six-coordinate variation on structure 1a in which two Si−O(H)••Cr linkages were imposed to complete the coordination sphere. The only structure that refined successfully, based on lowest residual and logical backscatter distances R, Debye−Waller factors, σ^2, was (≡SiO)$_2$Cr(═O)$_2$, Figure 1a, with no structure of higher coordination number ever yielding a fit with reasonable distances and/or Debye−Waller values (Supporting Information). Initial trial structures of Figure 1a utilized bond lengths and angles obtained from density functional optimized clusters reported by Dines and Inglis (Table 3, ref 6). When coordination numbers were freely refined, obtained values were close to integer values. To give physical meaning to the Debye−Waller factors, the coordination numbers were subsequently fixed. Fit parameters of model 1a to the k^3-weighted data are presented in Table 1.

The bond lengths determined from the fit are 1.60 and 1.80 Å (±0.02 Å) for the terminal and bridging bonds, respectively. These values are slightly longer than those obtained for the molecular analogue, [Cr(═O)$_2${OSiPh$_2$)$_2$O}]$_2$, 1.579 Å for Cr═O and 1.724 Å for Cr−OSi, or the corresponding silsesquioxane, [(c-C$_6$H$_{11}$)$_7$Si$_7$O$_{11}$(OSiMe$_3$)-CrO$_2$], 1.557, 1.574 Å for Cr═O and 1.730, 1.731 for Cr−OSi.[25,26] The distance of the terminal chromium−oxo bond, 1.60 Å, is slightly longer than the molecular analogues but within experimental uncertainty, ±0.02 Å. The Debye−Waller factor of 0.00456 Å^2 is reasonable, indicating that the two oxos are similarly bound. The terminal Cr−siloxide distance obtained from the EXAFS fits is slightly elongated from molecular analogues ∼1.73 Å and Dines and Inglis calculation of 1.74 Å.[6] The Debye−Waller factor of 0.00785 Å^2 suggests some variability and/or asymmetry between the individual (≡SiO)$_2$Cr(═O)$_2$ units or between the chromium−siloxide bonds on *each* subunit. However, it is difficult to distinguish two individual Cr−OSi paths which vary from each other by less than 0.12 Å.[27] The elongation and uncertainty in the chromium−siloxide bond length may have an electronic origin; however, more likely it reflects micro-

(23) Arcon, I.; Mirtic, B.; Kodre, A. *J. Am. Ceram. Soc.* **1998**, *81*, 222−224.
(24) Pak, C.; Haller, G. L. *Microporous Mesoporous Mater.* **2001**, *48*, 165−170.
(25) Abbenhuis, H. C. L.; Vorstenbosch, M. L. W.; van Santen, R. A.; Smeets, W. J. J.; Spek, A. L. *Inorg. Chem.* **1997**, *36*, 6431−6433.
(26) Feher, F. J.; Blanski, R. L. *J. Chem. Soc., Chem. Commun.* **1990**, 1614−1616.
(27) Given the formula $\Delta R = \pi/2\Delta k$, where Δk is the data range in k space and ΔR is the effective resolution between two identical backscatters. See: Riggs-Gelasco, P. J.; Stemmler, T. L.; Penner-Hann, J. E. *Coord. Chem. Rev.* **1995**, *144*, 245

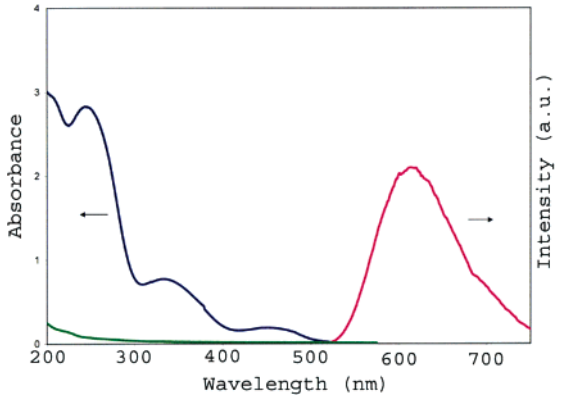

Figure 3. Photoemission spectrum (red) and electronic absorption spectra of a 0.005 mol % Cr (blue) and pure silica (green) xerogel.

scopic variability of the silica surface, which will impose a distribution of lengths and angles on the Cr−siloxide linkage.

Significant intensity is apparent at ∼3 Å in *R* space of the k^3-weighted EXAFS, Figure 2b. If present, Cr−Cr interactions would be enhanced by collection of the data at cryogenic temperatures.[28,29] This is not the case here as attempts to refine a Cr backscatter to this intensity were unsuccessful. By examining the imaginary component of the EXAFS at ∼3 Å, we conclude that a Cr−Cr interaction is unlikely (Supporting Information) due to the antiphase behavior of the Cr−Cr path relative to the data. Additionally, silicon backscatters were not conclusively detected in the second coordination sphere. Fits that included a Cr−Si path ($N = 2$) returned a plausible distance ($R = 3.18$ Å) and were more consistent with the imaginary EXAFS (Supporting Information) but returned a large Debye−Waller factor ($\sigma^2 = 0.01638$ Å^2). As the inclusion of the Cr−Si path was not statistically warranted by the *F* test, the distance of 3.18 Å should not be regarded as reliable. Similar attempts were made to refine multiple-scattering pathways to gain bond-angle information for the O═Cr═O and SiO−Cr═O bonds as these paths are likely the cause of the intensity at ∼3 Å. However, these did not yield meaningful results. To the best of our knowledge, this is the best structural refinement of EXAFS data for Cr(VI) on silica. This refinement and the failure to achieve refinement with other plausible structures give strong support to the dioxo structure.

Raman Spectroscopy of the Cr(VI) Site. The electronic spectrum of highly dilute Cr(VI) dispersed in a silica xerogel monolith and collected in transmission mode through the monolith is shown in Figure 3. Three relatively intense LMCT bands occurring at [$\lambda(\epsilon)$] 450(510), 332(2053), and 241(7470) nm are observed in the absorption spectrum. The Cr(VI) site also shows a strong red luminescence commencing at ∼525 nm and centered at 617 nm.[30] The strong electronic absorptions throughout the visible coupled with the intense luminescence create difficulty in collecting Raman spectra. Most commonly used visible excitation wavelengths will be exciting electronic transitions and, hence,

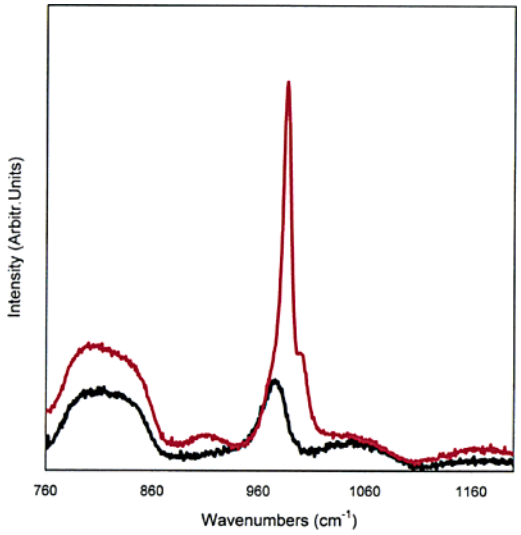

Figure 4. Raman spectra of a 0.5 mol % Cr−silica xerogel (red) and a pure silica xerogel (black) collected at 784.5 nm.

subject to self-absorption. Unless the wavelength chosen is sufficiently short that the Raman scattering can be collected before the onset of emission the luminescence will obscure all but the most intense features. Spectra in earlier studies by Wachs et al. and more recent study by Dines and Inglis were collected by exciting into the first electronic transition, and all show obfuscation of the Raman scattering from the Cr luminescence.[3,4,6]

Figure 4 shows the Raman spectrum of a dilute (0.5 mol %) Cr(VI)−silica xerogel collected off resonance by excitation at 784.5 nm. Since the excitation is at a longer wavelength than the first absorption there is no fluorescent background and vibrational modes related to the chromium are clearly resolved. The spectrum, when compared to pure silica (Figure 4), shows several features attributable to the Cr site. An intense, well-resolved band is observed at 986 cm^{-1}, and to the high-energy side, existing as a resolved shoulder, is a peak at ∼996 cm^{-1}. Comparison with a pure silica xerogel (Figure 4) shows that both of these modes are convoluted with the symmetric $(-O)_3Si-OH$ stretch of the pure silica xerogel lying at 980 cm^{-1} and the low-energy side of the broad transverse-optical (TO) antisymmetric stretch of the silica network lying at ∼1050 cm^{-1}.[31−34] One other band that can be assigned with certainty to the Cr site is a weak broad feature at ∼919 cm^{-1} that has no counterpart in the pure silica control spectrum. The spectrum can be deconvoluted (Figure 5) into its constituent spectroscopic peaks with considerable accuracy (i.e., no unresolved or spurious peaks were generated in the deconvolution routine). The deconvolution places the peak maxima of the three Cr features at 919, 986, and 1001 cm^{-1}. The intense 986 cm^{-1} band is the symmetric Cr═O stretch that has been assigned previously. In recent work by Dines and Inglis, density functional calculations of model complexes assigned the 1001 cm^{-1} transition to the previously unresolved antisymmetric

(28) Barnes, C. E.; Ralle, M.; Vierkotter, S. A.; Penner-Hann, J. E. *J. Am. Chem. Soc.* **1995**, *117*, 5861−5862.
(29) Barnes, C. E.; Shin, Y.; Saengkerdsub, S.; Dai, S. *Inorg. Chem.* **2000**, *39*, 862.
(30) Hazenkamp, M. F.; Blasse, G. *J. Phys. Chem.* **1992**, *96*, 3442−3446.
(31) Galeener, F. L. *Phys. Rev. B* **1979**, *19*, 4292−4297.
(32) Galeener, F. L.; Leadbetter, A. J.; Strongfellow, M. W. *Phys. Rev. B* **1983**, *27*, 1052−1078.
(33) Galeener, F. L.; Mikkelsen, J. C. *Phys. Rev. B* **1981**, *23*, 5527−5530.
(34) Sen, P. N.; Thorpe, M. F. *Phys. Rev. B* **1977**, *15*, 4030−4038.

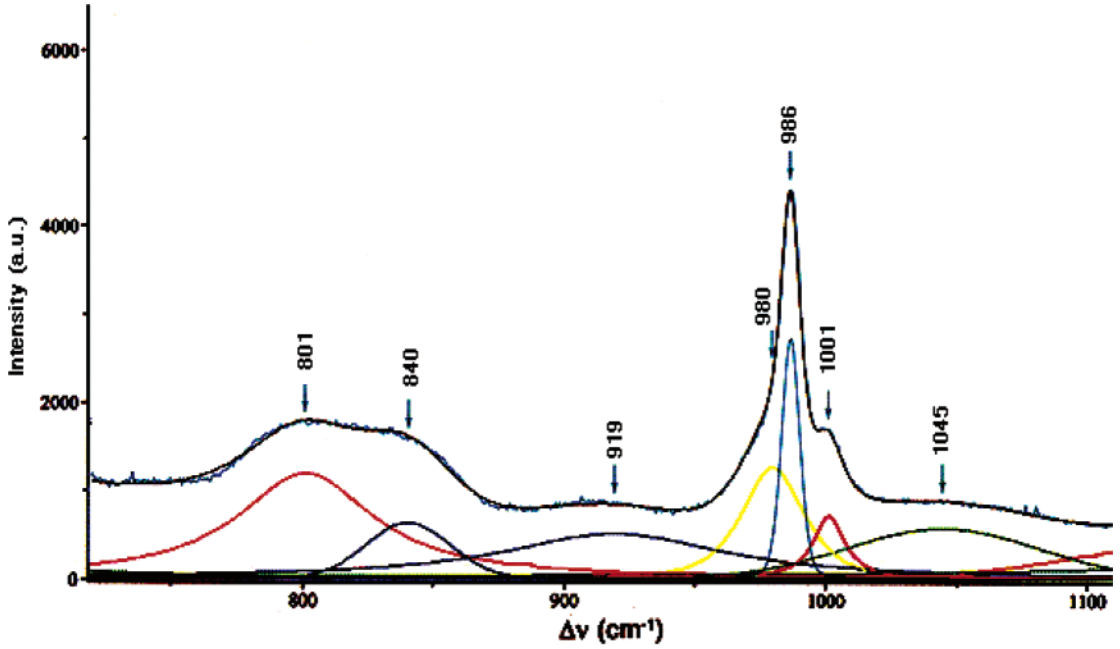

Figure 5. Raman spectra of a 0.5 mol % Cr−silica xerogel collected at 784.5 nm showing Gaussian−Lorentzian deconvolution into contributing spectral bands.

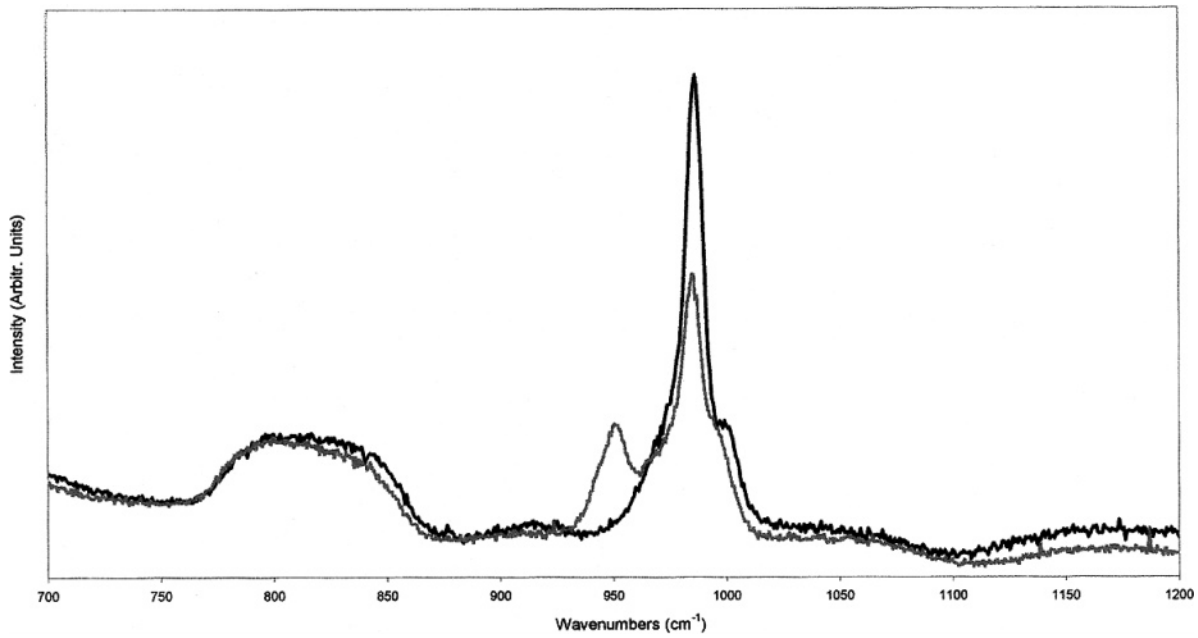

Figure 6. Raman spectra of a 0.5 mol % Cr−silica xerogel before (black) and after (gray) three cycles of reduction/oxidation in the presence of $^{18}O_2$ collected at 784.5 nm.

CrO_2 stretch and, similarly, the 919 cm^{-1} transition to a Si−O−Cr mode coupling the Cr to the silica network.[6] Both are reasonable assignments though the bridging stretch is significantly lower in energy than other M−O−Si stretches in amorphous silica such a V−O−Si and Ti−O−Si which occur at ∼930 and 947 cm^{-1}, respectively.[12,13,35,36] The low frequency is probably due, at least in part, to the increased mass of the CrO_2 unit and that it is connected by only two bonds to the silica surface. Bands to higher frequency would not be expected for the Cr site and none are observed, with silica features obscuring any bands present at lower frequency.

Insertion of ^{18}O into the coordination sphere of a 0.5 mol % Cr−silica xerogel was achieved by first reducing the Cr sites with CO at 230 °C followed by reoxidation at 530 °C in $^{18}O_2$ at 125 psi. Repetition of the reduction−oxidation cycle was carried out five times, but after the third cycle only modest changes in the spectra were observed (Figure 6). The sequential redox process used to incorporate ^{18}O into the coordination sphere of the Cr can, in principle, replace any of the oxygens in the coordination sphere. As far as the terminal oxo groups are concerned, the significant amounts of unlabeled chromophore remaining after the redox process

(35) Moisii, C.; Curran, M. D.; van de Burgt, L. J.; Stiegman, A. E. *J. Mater. Chem.* **2005**, *15*, 3519−3524.
(36) Rice, G. L.; Scott, S. L. *J. Mol. Catal. A* **1997**, *125*, 73−79.

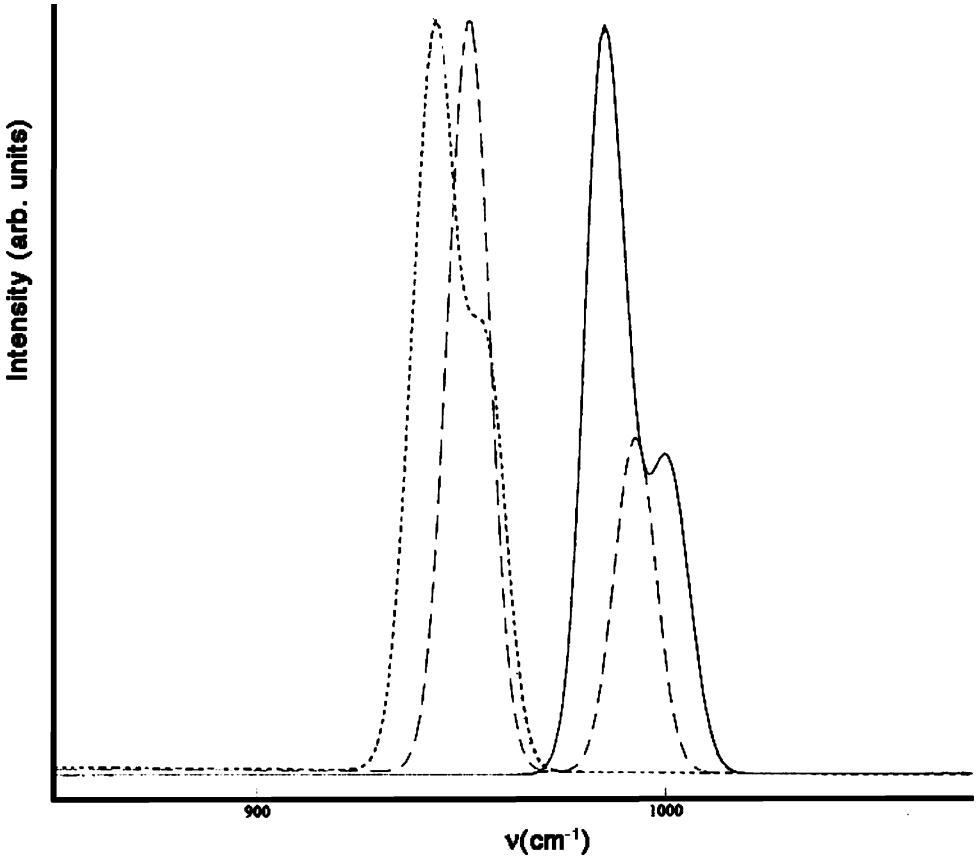

Figure 7. Predicted Raman spectra from normal-mode analysis of a $(Si-O-)_2CrO_2$ structural unit with various degrees of ^{18}O incorporation in the terminal bonds: (—) $Cr(=O^{16})_2$, (- - -) $Cr(=O^{16})(=O^{18})$. and (· · ·)$Cr(=O^{18})_2$.

suggest that the predominant species will be one that is partially substituted, i.e., $^{18}O=Cr=O^{16}$. Figure 7 shows the spectral changes in the symmetric and antisymmetric stretches, predicted from a normal-mode calculation of the $(-Si-O)_2Cr(=O)_2$ structural unit, for partial and total replacement of the terminal oxygens. The calculations predict a large shift of the symmetric stretch to 951 cm^{-1} and a modest change in the antisymmetric stretch to 992 cm^{-1}. The Raman spectrum of the ^{18}O-labeled material (Figure 6) shows the disappearance of the symmetric stretch at 986 cm^{-1} and the concomitant appearance of a band at 950 cm^{-1}. The magnitude of the shift is close to the value observed by Wachs et al. for higher loadings of Cr and agrees well with the prediction from the normal-mode calculation.[5,37] Calculations of the isotopic shift of the completely substituted $Cr(=O^{18})_2$ site predict that the symmetric and antisymmetric stretches will occur at 943 and 955 cm^{-1}, respectively (Figure 7). No peaks are resolved in this region, but a small amount of the completely labeled sites may account for some broadness in the low-energy side of the 950 cm^{-1} band.

The presence of a band assignable to the ^{18}O-labeled antisymmetric stretch is not obvious in the spectrum though, as indicated by its predicted position (Figure 7), it will overlap considerably with the remaining ^{16}O bands. Scrutiny of the changes in the unlabeled bands upon isotopic substitution reveals that the intensity of the symmetric 986 cm^{-1} mode decreases by about one-third with the three cycles of isotopic substitution. The 1001 cm^{-1} peak is no longer clearly resolved though a shoulder still exists at ~998 cm^{-1} consistent with the modest isotopic shift predicted for the antisymmetric stretch. One thing that is clear from the isotopic substitution is that the shifts are entirely consistent with the dioxo structure since a single terminal oxo species would show a much larger isotopic shift. Finally, the weak broad band centered at ~919 cm^{-1}, which is assigned to the bridging Cr−O−Si stretch, appears to get weaker and broaden out with ^{18}O substitution, but the resolution is insufficient to deduce whether the magnitude of the shift is consistent with substitution into the interfacial site.

An advantage to sol−gel synthesis is that homogeneous, transparent xerogels with a range of Cr concentrations can be prepared. As the Cr concentration increases, the amount of Cr−O−Si linkages will increase and self-condensation to form Cr−O−Cr linkages may also become observable. As such, systematic changes in the Raman spectrum as a function of concentration will both reinforce the assignment of modes associated with the isolated Cr sites and allow observation and assignment of bands associated with oligomer formation.

Raman spectra of a series of Cr−silica xerogels of increasingly larger Cr incorporation are shown in Figure 8. As the concentration increases, the symmetric CrO_2 stretch becomes systematically more intense, notably, however, it remains at approximately the same frequency at 5 mol %. The bandwidth varies only slightly over the range with an

(37) Czernuszewicz, R. S.; Spiro, T. In *Inorganic Electronic Structure and Spectroscopy*, 1st ed.; Solomon, E. I., Lever, A. B. P., Eds.; Wiley: New York, 1999; Vol. 1, p 732.

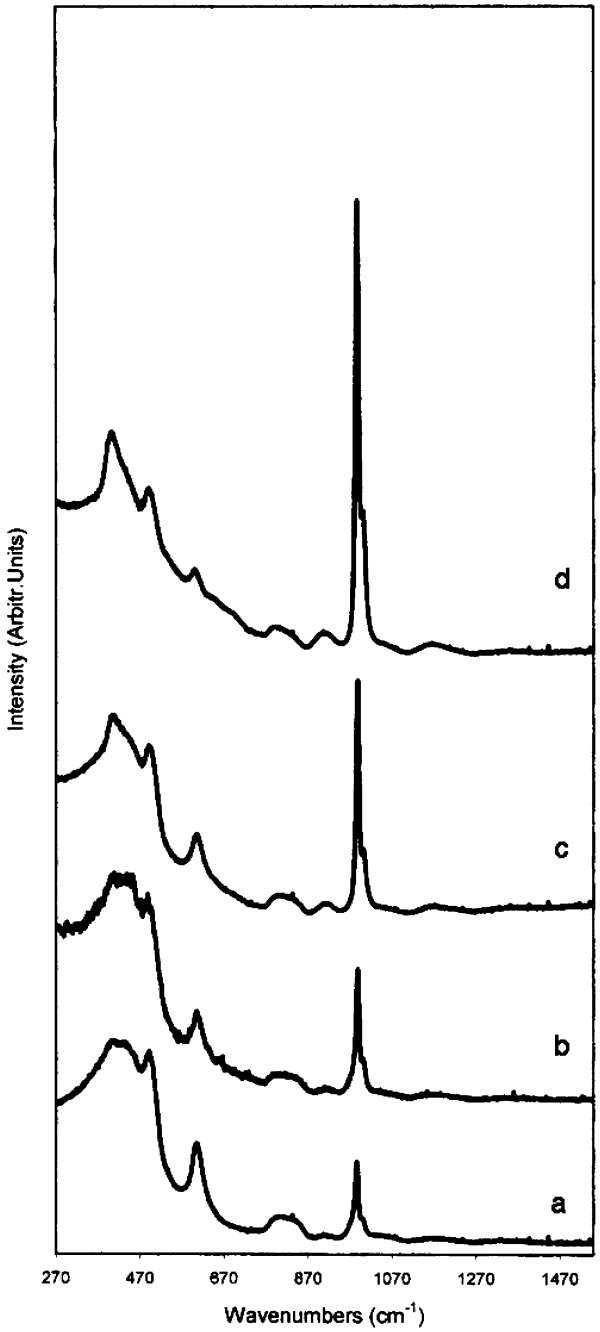

Figure 8. Raman spectra of (a) 0.5, (b) 1.0, (c) 2.0, and (d) 5.0 mol % Cr−silica xerogel collected at 784.5 nm excitation.

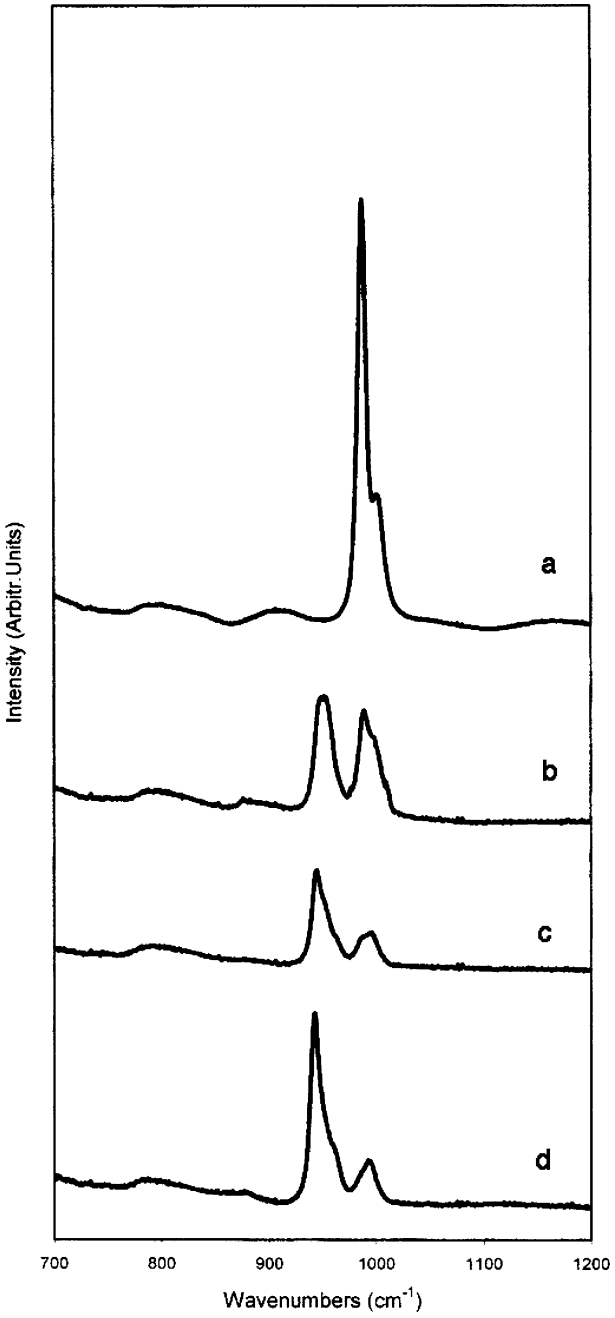

Figure 9. Raman spectra (784.5 nm excitation) of a 5.0 mol % Cr−silica xerogel (a) before and after (b) one, (c) four, and (d) five cycles of reduction followed by oxidation with $^{18}O_2$.

average fwhm of 9.1 ± 0.4 cm^{-1} for the entire series. The shoulder, which is better resolved in the more concentrated sample, occurs at 1004 cm^{-1} and has an intensity relative to the 986 cm^{-1} mode that is virtually identical to what it is in the dilute sample and, in fact, is constant over the entire concentration range with an average I_{1004}/I_{986} ratio of 0.45 and a standard deviation of 12%. The constancy of this ratio indicates that the 1004 cm^{-1} band is related, either directly or indirectly, to the presence of the Cr in the matrix. The band at 919 cm^{-1}, which has been tentatively assigned to the Cr−O−Si stretch, grows in intensity with increasing concentration with its intensity relative to the 986 cm^{-1} band remaining reasonably constant; however, due to the weakness and broadness of the 919 cm^{-1} band the correlation is poorer. At higher concentration, other bands begin to be resolved below 700 cm^{-1}. In particular, sharp bands are observed in the 5 mol % sample at 602, 492, and 404 cm^{-1}. Unambiguous assignment of bands in this region at higher loadings of metal ions is difficult as silica-based modes associated with the breakdown of the silica network appear along with discrete and oligomeric peaks associated with the increasing metal concentrations.[38, 39]

The results of sequential ^{18}O labeling of the 5 mol % sample on its Raman spectrum are shown in Figure 9. After the first reduction/oxidation cycles the symmetric stretch shows an isotopic shift to 951 cm^{-1}, which corresponds well

(38) Brawer, S. A.; White, W. B. *J. Chem. Phys.* **1975**, *63*, 2421−2432.
(39) Furukawa, T.; Fox, K. E.; White, W. B. *J. Chem. Phys.* **1981**, *75*, 3226−3237.

to the value predicted for partial substitution of the Cr site ($^{16}O{=}Cr{=}O^{18}$). The isotopically shifted band is broad (fwhm = 16 cm^{-1}), which probably reflects increased contribution from complete, $^{18}O{=}Cr{=}O$,^{18} isotopic enrichment. As with the dilute material, no peak directly assignable to the ^{18}O-labeled antisymmetric stretch is observable in the spectrum; however, the peak broadness and spectral congestion could prevent resolution of the peak. Notably, in these early stages of substitution the rate of disappearance of the 986 and 1004 cm^{-1} bands differs, which suggests that they are not the symmetric and antisymmetric components of the same stretch; however, due to the potential emergence of bands in this region due to isotopic substitution, this observation should be taken with some caution. After the fifth reduction/oxidation process a significant amount of the Cr sites have been substituted with ^{18}O as evidenced by the low relative intensity of the remaining 986 cm^{-1} band. The symmetric stretch now has a peak maximum at 943 cm^{-1}, which is the predicted value for completely substituted dioxo sites [$Cr(=O^{18})_2$]. Also observed is a shoulder which, upon deconvolution, has a peak maximum of 954 cm^{-1}, very close to the predicted value for the antisymmetric stretch. However, this interpretation must be taken with some caution because of possible interference from the intense symmetric stretch of remaining $^{16}O{=}Cr{=}O^{18}$ species.

Definitive information about the symmetry of the high-energy shoulder is obtained from the polarization ratios, which can be obtained with considerable accuracy in the monolithic xerogels. The parallel and perpendicularly polarized Raman spectrum of a 0.5 mol % Cr−silica xerogel is shown in Figure 10. As can be seen in the spectrum, both the 986 and 1001 cm^{-1} bands are strongly polarized. The polarization ratio, $I_\perp/I_{II}$, taken from the areas of the 986 cm^{-1} peak deconvoluted from the high energy is 0.36, consistent with its assignment as the symmetric CrO_2 stretch. More significantly, the polarization ratio for the 1001 cm^{-1} band is 0.43, which is so small that it cannot be realistically assigned to the antisymmetric $Cr(=O)_2$ stretch. In short, for discrete isolated Cr sites on silica, the high-energy band appearing as a shoulder on the symmetric stretch cannot be reliably assigned to the antisymmetric component of the CrO_2 group.

This observation leads to the question of why the antisymmetric mode for the CrO_2 dioxo group is not observed and what the nature of the 1001 cm^{-1} shoulder is. Given the general veracity of the Dines and Inglis calculation in predicting other modes from the CrO_2 unit, it is likely that the antisymmetric stretch occurs in this spectral region. Failure to observe the antisymmetric stretch, particularly at low concentrations, may be due to its inherent weakness, which makes it unobservable above the silica features. In chromyl fluoride the symmetric and antisymmetric chromium−oxygen stretches occur at 995 and 1045 cm^{-1}, respectively, but the antisymmetric stretch has an intensity that is only 2% of the symmetric stretch.[40] Since the silica environment is electron withdrawing, metal oxide sites of high-valent first-row transition metals are likely to be poorly polarizable with the antisymmetric modes being the weakest scatterers. In fact, in studies of V(V) and Ti(IV) dispersed in amorphous silica the only metal-localized antisymmetric stretch observed is the Ti−O−Si mode at ∼945 cm^{-1}.[13,35,41] These bands may become observable on other, less electron withdrawing supports and may suggest that additional care should be exercised in comparing Raman spectra of a specific catalytic site across different supports.

Since the primary terminal stretching mode of the CrO_2 unit remains virtually unchanged as the concentration of Cr increases, evidence for the antisymmetric stretch may become

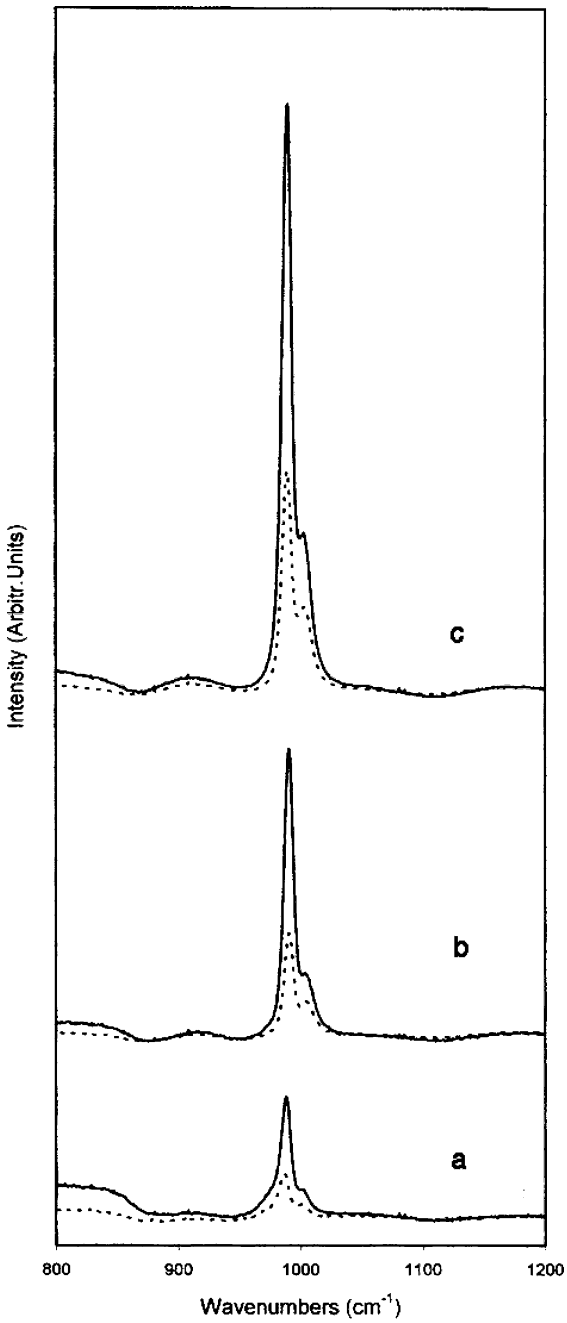

Figure 10. Raman spectra with Raman scattering collected polarized parallel (—) and perpendicular (- - -) to the incident polarization for (a) 0.5, (b) 2, and (c) 5.0 mol % Cr−silica xerogel.

(40) Brown, S. D.; Gard, G. L.; Loehr, T. M. *J. Chem. Phys.* **1976**, *64*, 1219−1222.

(41) Knight, D. S.; Pantano, C. G.; White, W. B. *Mater. Lett.* **1989**, *8*, 156−160.

(42) Vaarkamp, M. *Catal. Today* **1998**, *39*, 271−279.

observable at its correct position at higher concentrations. For 2 and 5 mol % the parallel and perpendicular polarizations are shown in Figure 10b an 10c. As is evident in the spectra, the high-energy shoulder is better resolved in the perpendicular polarization of the higher concentration sample and has a peak maximum of 1004 cm^{-1}. The polarization ratio for the 987 cm^{-1} symmetric mode is relatively unchanged and has a value of 0.35 and 0.36 for the 2 and 5 mol %, respectively. The high-energy shoulder is less strongly polarized with a value of 0.74 for the 2 mol % sample and then declines again to 0.52 for the 5 mol % sample. While the 5 mol % sample is still fairly strongly polarized, the 2 mol % sample is at a value that is ambiguous but probably reflects a contribution from the antisymmetric mode.

Since modes that have weak Raman scattering are often intense in the infrared, it may be possible to observe the antisymmetric mode in the infrared provided they are not obscured by the intense silica transitions. FT-IR spectra collected as diffuse reflectance spectra of a 5 mol % Cr in silica are shown in Figure 11. The spectra reveal no bands that can be assigned to either of the CrO_2 stretching modes emerging from the silica envelope. Isotopic substitution in an effort to shift the transitions into the transparent window below 950 cm^{-1} was also not successful, though a broadening of the low-energy side of the spectral envelope is observed. The band assigned to the Si−O−Cr stretch is easily observed at 913 cm^{-1} in the IR. It exhibits an isotopic shift of 33 cm^{-1}, consistent with its assignment as a bridging mode.[3]

Clearly, the isotopic labeling and polarization studies do not support the straightforward assignment of the 1004 cm^{-1} Raman band to the antisymmetric stretching mode of the CrO_2 unit. Since the antisymmetric stretch of small molecule analogues such as CrO_2F_2 are strongly nonpolarized ($I_\perp/I_{II} = 0.93$) the lack of a well-defined unpolarized mode in the Cr−silica materials must be related to aspects of the Cr−silica system as a whole.[40] One possibility is that the band is the antisymmetric stretch but that the C_{2v} site symmetry is significantly broken at the interface of the silica surface, thereby making the mode symmetric. Certainly the EXAFS data indicates an uncertainly in the Si−O−Cr bond lengths due to disorder at the surface, which lends support to this argument. However, if this symmetry breaking mechanism were the only cause for polarization of the band, then its value would be expected to remain constant as a function of concentration as observed for the symmetric stretch (at least over the lower concentration range before the onset of significant oligomerization). In fact, the decrease in the polarization ratio at high (5 mol %) concentrations may be the result of significant symmetry breaking due to oligomerization. As suggested previously, the antisymmetric stretch may be very weak and evidence of it may not appear until higher Cr concentrations are reached. Inherent weakness in its intensity is consistent with the observed increase in the polarization ratio at higher Cr loadings, which suggests it is convoluted with another mode which is the resolved shoulder seen at low concentrations. The nature of this transition may be related to the disrupted silica network in the proximity of the Cr site. A similar band is observed in silica-supported vanadium oxide where a resolved shoulder at 1059 cm^{-1} lies on the high-energy side of the intense terminal V═O stretch at 1039 cm^{-1}. As in the case of Cr, the shoulder is highly polarized and its intensity, relative to the V═O stretch, tracks with metal ion concentration.

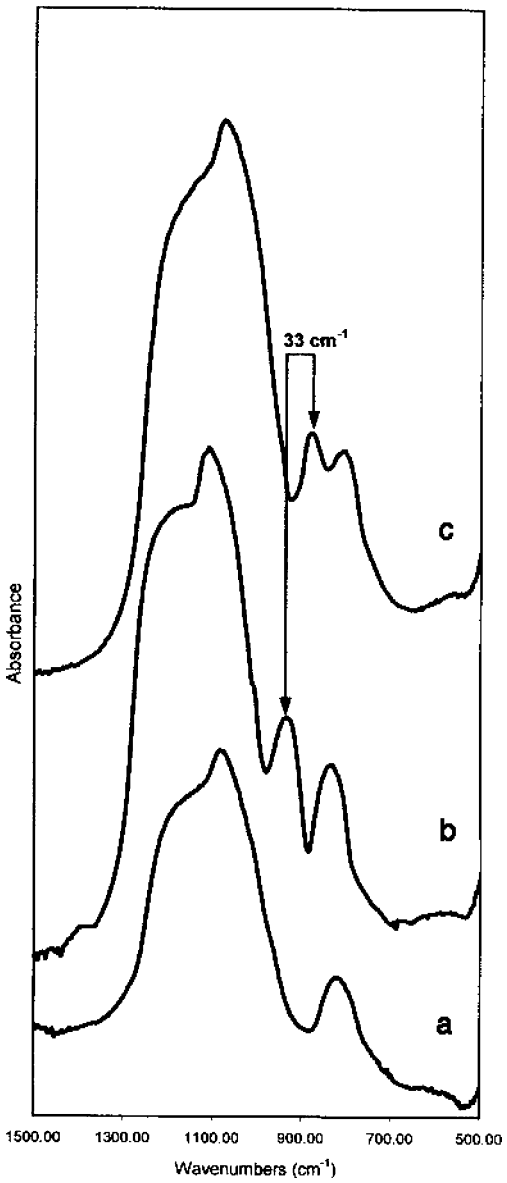

Figure 11. FT-IR of pure silica (a) and 5 mol % (b) ^{16}O Cr−silica and (c) ^{18}O Cr− silica xerogel

In conclusion, this study has shown through EXAFS analysis that the discrete Cr(VI) sites dispersed in silica have the dioxo structure that is usually postulated. The bond lengths refined in the EXAFS structure compare well with those found from density functional calculations of model cluster complexes. Raman spectroscopy of the site unambiguously shows that, for discrete isolated Cr sites, all of the observed Raman bands associated with the Cr are totally symmetric and that the antisymmetric $Cr(=O)_2$ stretch is not observed. At higher Cr concentrations ^{18}O labeling and polarization studies indicate that the antisymmetric mode is present though probably overlapping with other vibrational modes. These results suggest that while careful calculation

can provide a valuable guide to the energies of vibrational modes, spectroscopic techniques are required to unambiguously assign observed transitions.

Acknowledgment. Funding was provided by the Air Force Office of Scientific Research through MURI 1606U81. We thank Prof. Trevor Dines for helpful comments and Dr. Eric Dowty of Shape Software for helpful discussions.

Supporting Information Available: Three additional figures and three tables. This material is available free of charge via the Internet at http://pubs.acs.org.

CM0601281